

PORO-FRACTURE ANALYSIS OF CONCRETE USING A DAMAGE MECHANICS MODEL

S.S. Bhattacharjee, F. Ghrib, R. Tinawi, and P. Léger
Department of Civil Engineering, École Polytechnique
Montreal, Québec, Canada

Abstract

The continuum description of concrete fracture response is very efficient for practical applications in the safety assessment of large mass concrete structures. A poro-damage constitutive model is presented in this paper, with a direct dependence between the state of damage evolution and the pore-pressure inside the fracture process zone. Experimental results published in the literature, on the water-fracture interaction effects in concrete specimens, are considered to validate the numerical implementation. The proposed model may be used to analyse concrete dams, where the permeability of the intact concrete is low, and the water pressure effects are generally confined within the construction joints and the fracture process zone of newly evolving crack profiles.

1 Introduction

The poro-fracture modelling of concrete is an indispensable part of the safety assessment of water retaining structures. Cracks that originate on the upstream face of a structure are subjected to additional loading effects

due to the intrusion of water. The mechanical load effects of pore water, often referred to as the ‘uplift pressure’, can be considered in a finite element analysis by using the standard effective stress concept. However, the permeability change during the evolution of damage modifies the internal pressure, and this in turn influences the deformation response of the system. Special numerical algorithms are required to model this coupled poro-fracture response of structures. In addition to this mechanical coupling effects, the presence of pore water pressure may cause micro-structural damage in the fracture process zone (FPZ), with an apparent reduction of the specific fracture energy of concrete (Brühwiler and Saouma 1991). Several researchers have considered the mechanical effects of water pressure in discrete crack models (Reich et al. 1994, Gioia et al. 1992, Brühwiler and Saouma 1991, Amadei et al. 1991, Ingraffea 1990, Linsbauer et al. 1989, Ayari 1988). Continuum models of the poro-fracture response have been used by others, based on plasticity (Fauchet et al. 1991), damage mechanics (Bourdarot and Barry 1994), and smeared fracture concepts (Bhattacharjee and Léger 1995).

The continuum description of concrete fracture response is very appealing for its computational efficiency, and for its scopes to include other constitutive aspects of the material behaviour. The objective of this paper is to develop a numerical analysis tool that considers the fundamental aspects of poro-fracture behaviour in a simplified way to render practical applications in structural safety assessment. The softening behaviour in the concrete fracture process zone is represented as a loss of contact area, which results in a degradation of the elastic stiffness. The fracture energy conservation principle is used to define the evolution of elastic damage. The water pressure inside the FPZ is defined directly in terms of the damage state variable and the effective porosity of the material. An iterative analysis technique is adopted to simulate the water-fracture interactions in the FPZ. Experimental results on the water-fracture interaction in concrete specimens, reported by Brühwiler and Saouma (1991), are considered to validate the computational model. Different features of the poro-damage model, that has been implemented in the FRAC_DAM computer program (Bhattacharjee 1995), are presented in the following sections.

2 Numerical simulation of the poro-fracture response

The system of equations for a static deformation response and a steady state pressure response can be expressed as:

$$\begin{aligned} [K]\{u\} - [Q]\{p\} &= \{f\} & (a) \\ [H]\{p\} &= \{q\} & (b) \end{aligned} \quad (1)$$

where $[K]$ is the stiffness matrix of the structure; $[Q]$ is the matrix that couples the pressure field with the displacement field; $[H]$ is the permeability matrix; $\{f\}$ is the mechanical load vector; $\{q\}$ is the vector of fluid flow; and $\{u\}$ and $\{p\}$ are respectively the nodal displacement and pressure response vectors. During the nonlinear stress-deformation response of a system, the permeability matrix $[H]$ will change. Equations (1b) can be solved to obtain the nodal pressure values, and that can be subsequently applied to solve the stress equilibrium equations (1a).

Instead of solving the global equilibrium equations of fluid flow (Eqn. 1b), the change in pressure field, $\{p\}$, due to concrete cracking and structural joint opening, can be explicitly defined based on the past numerical experiences and experimental observations (Brühwiler and Saouma 1991; Amadei et al. 1991). The explicitly defined pressure data is used as an input to the stress equilibrium equations (1a), and the unknown displacement response is computed. The pressure field can be updated depending on the displacement response, and an iterative solution strategy is required to achieve convergence. In the context of concrete dam analysis, several investigators have used this technique for known location and orientation of cracks and joints (e.g. Reich et al. 1994). In this paper, a similar strategy is used with a poro-damage model, that can be used when the crack location and orientation are not known *a priori*. The porosity and the pressure in the material are expressed as functions of the scalar damage index.

3 Damage mechanics model of concrete

The damage process in concrete initiates from the micro-mechanical defects, and the coalescence of micro-cracks leads to the material failure with a macroscopic localization of the deformation field. The authors have previously developed orthotropic damage simulation models based on the elastic stiffness degradation and damage mechanics concepts, to investigate the static and seismic fracture responses of unreinforced concrete dams (Ghrib and Tinawi 1995, Bhattacharjee and Léger 1995). For the stated objective of this paper, an isotropic damage mechanics model is considered, which provides a simplified frame-work to investigate the poro-fracture behaviour of concrete. The damage evolution law of this model is similar to the one presented by Cervera et al. (1992).

The constitutive relations of an isotropic continuum are expressed as:

$$\{\sigma\} = [C(d)] \{\epsilon\} = (1-d) [C]_0 \{\epsilon\} \quad (2)$$

where $\{\sigma\}$ and $\{\epsilon\}$ are the stress and strain vectors respectively; $[C]_0$ is the elasticity matrix of the virgin material; and d is a scalar index of the

accumulated damage in the material ($0 \leq d \leq 1$). The evolution of d is defined based on the deformation state, that is expressed by an equivalent strain of the continuum as follows:

$$\epsilon_{eq} = \left(\kappa + \frac{1-\kappa}{m} \right) \sqrt{\frac{1}{E_0} \cdot \{\epsilon\}^T \cdot [C]_0 \cdot \{\epsilon\}} \quad ; \quad \kappa = \frac{\sum_{i=1}^3 \langle \sigma_e^i \rangle}{\sum_{i=1}^3 |\sigma_e^i|} \quad (3)$$

where E_0 is the Young's modulus of the virgin material; m is the ratio between compressive and tensile strengths of concrete; κ is the weighted average of the tensile stress amplitude; and σ_e^i ($i=1,2,3$) are the principal stresses if the material were in an undamaged state, $\{\sigma\}_e = [C]_0 \{\epsilon\}$. The damage process initiates when ϵ_{eq} exceeds the initial threshold, ϵ_0^t :

$$\epsilon_0^t = \frac{f_t}{E_0} \quad (4)$$

where f_t is the uniaxial tensile strength of concrete. At the post-elastic state, the new threshold (ϵ_i^t) is set to the maximum deformation response, ϵ_{eq} , that has been attained during the past loading history. Using an exponential degradation form of the elastic properties, and the principle of conservation of fracture energy, the evolution of damage is expressed as:

$$d = 1 - \left(\frac{\epsilon_o^t}{\epsilon_i^t} \right) \text{EXP} \left[A \left(1 - \frac{\epsilon_i^t}{\epsilon_o^t} \right) \right] ; \text{ where, } A = \left(\frac{G_f E_0}{l_{ch} f_t^2} - \frac{1}{2} \right)^{-1} \geq 0 \quad (5)$$

Here G_f is the fracture energy of concrete, and l_{ch} is the width of the numerically simulated crack band. A schematic representation of the damage evolution law is shown in Fig. 1.

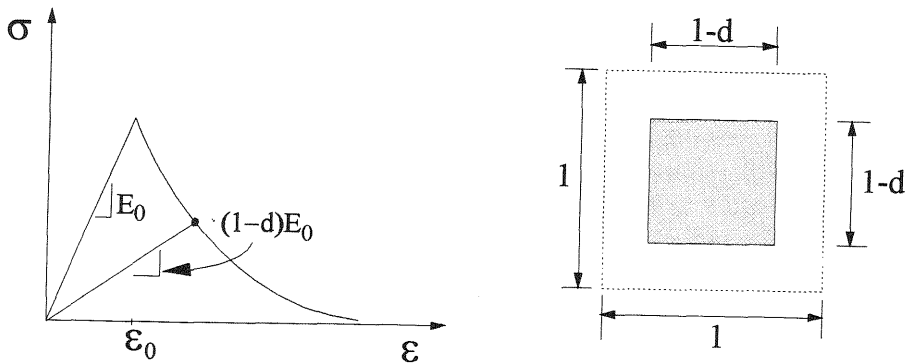


Fig. 1 Isotropic damage mechanics model

4 Poro-fracture interaction model

The micro-mechanical damage is assumed to be homogeneously distributed, and an isotropic poro-damage constitutive model is adopted to describe the stress-strain response of the porous media. The effective mechanical stress in the continuum, $\{\sigma\}$, is defined as follows (Fig. 2):

$$(1-d)\{\sigma\} = \{\sigma\}^t + \{b\}p \quad (6)$$

where $\{\sigma\}^t$ is the externally applied stress; p is the internal pore pressure; and $\{b\} = b\{1,1,1,0,0,0\}^T$ defines the effective porosity of the continuum, b ($0 \leq b \leq 1$) being the Biot coefficient. The effects of micro-mechanical damage on the pressure field of the continuum are expressed by the following two recursive expressions:

- The effective porosity of the material increases as:

$$b_i = b_{i-1} + (1-b_{i-1}) f_i(d) \quad (7)$$

- The internal pore-pressure p changes as:

$$p_i = p_{i-1} + (p_m - p_{i-1}) g_i(d) \quad (8)$$

where $i-1$ and i refer to two successive damage evolution steps; $f_i(d)$ [$0 \leq f_i \leq 1$] is a parameter that relates the effective porosity to the state of damage in the continuum; p_m is the maximum pressure that may develop at the completely damaged state; and $g_i(d)$ [$0 \leq g_i \leq 1$] represents the interaction between the state of damage and the fluid pressure inside the pores. The functions f_i and g_i may be intuitively defined, and their suitability can be verified by comparing the predicted responses with the experimental results. In the present numerical investigations, the rate of

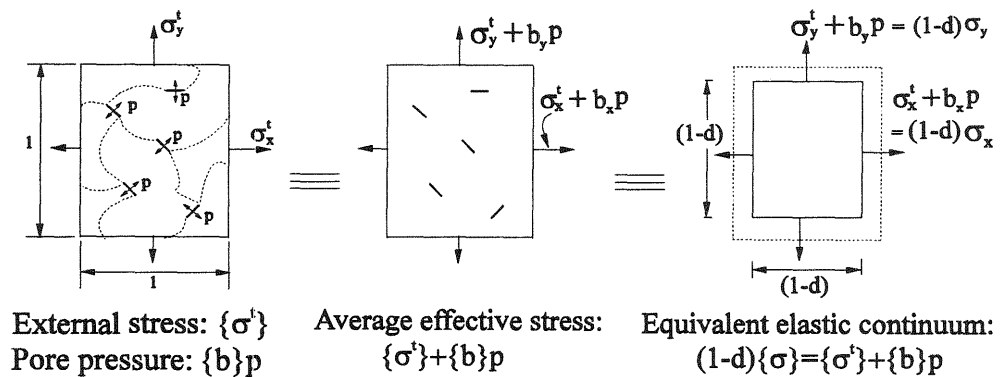


Fig. 2 Effective stresses in the saturated porous continuum

pore pressure change is related directly to the rate of material damage, and the following definition is adopted for both f_i and g_i :

$$f_i(d) = g_i(d) = \frac{\langle d_i - d_{i-1} \rangle}{1 - d_{i-1}} ; \quad (0 \leq d_{i-1} < 1) \quad (9)$$

At the initial state $d_{i-1}=d_0$, that specifies a threshold to initiate the pore-pressure changes. The water-fracture interaction model can be initiated simultaneously with the damage evolution by assigning $d_0=0$. A higher value can be assigned to induce a lag between the damage front and the water pressure front. The pressure at the beginning of the recursive analysis, p_0 , may be different from zero if an initial pore pressure exists at the elastic state of the material. Similarly the initial value of porosity may be set to the elastic Biot coefficient b_0 .

Equations (7)-(9) define the evolution of pore pressure in a damaged continuum. The pressure loads from finite element integration points are assembled to form the corresponding load vector in Eqn. (1) as follows:

$$[Q]\{p\} = \{f\}_p = \int [B]^T \{b\} p \, dV \quad (10)$$

where $[B]$ is the strain-displacement transformation matrix. An incremental iterative analysis algorithm is used to achieve convergence between the variable deformation field, $\{u\}$, the internal pressure load, $\{f\}_p$, and the external applied load $\{f\}$. The post-peak response of a structure is simulated by using an indirect displacement control algorithm, where the external load $\{f\}$ is adjusted based on a selected deformation response, e.g. the crack-mouth-opening-displacement (CMOD).

5 Numerical experiments

The wedge splitting concrete specimens, tested by Brühwiler and Saouma (1991), are considered in this study for numerical experiments. Laboratory tests were conducted without water pressure (Type I), and with water pressure (Type II) to determine its effects on the fracture properties of concrete. Type II experiments were initiated with mechanical loads (initial pore pressure, $p_0=0$), followed by a cyclic application and removal of the water pressure p_m through the initial notch. The specimens were eventually failed under mechanical loads only. Several experiments were conducted with different values of p_m : 0.1,0.3,0.5,0.7 and 0.9 MPa. Based on the experimental results, Brühwiler and Saouma (1991) suggested a reduction of the concrete fracture energy to take account of the additional micro-structural damage that might be caused by the pore water pressure. The objective of the present numerical experiments is to verify the necessity of adjusting the material fracture parameters, when the poro-

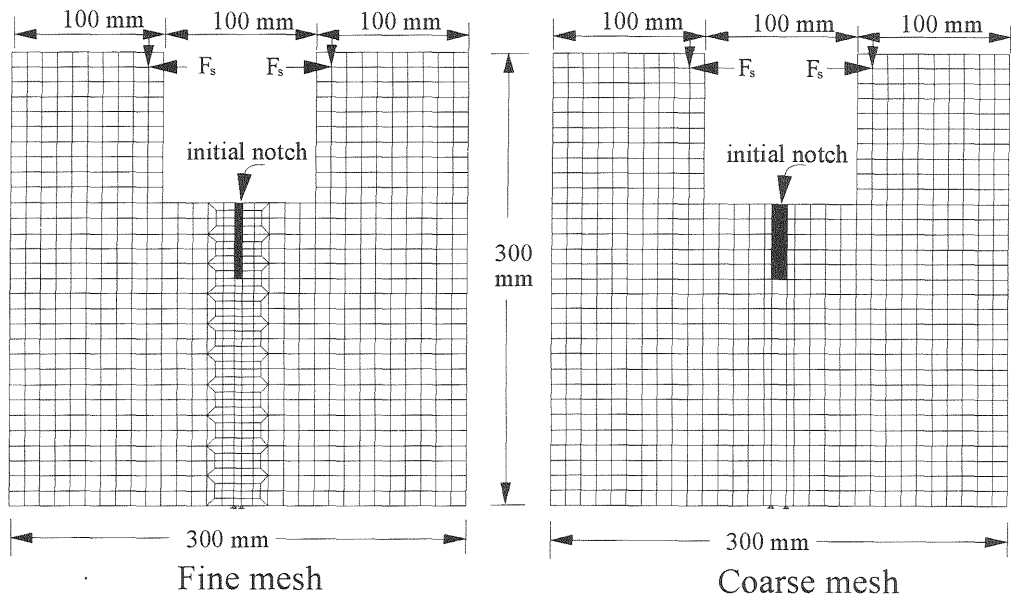


Fig. 3 Finite element models (thickness = 100 mm)

damage model is used to investigate the water-fracture responses of the concrete specimens.

Figure 3 shows two fine element meshes that are considered in the present investigations. The material properties used in the plane-stress analysis models are identical to those reported in the literature (Reich et al. 1994): $E_0 = 24320$ MPa, $\nu = 0.2$, $f_t = 2.54$ MPa, and $G_f = 182$ N/m. The poro-damage parameters are assumed to be $b_0 = d_0 = 0$.

5.1 Simulation of experimental results without water pressure

The Type I experiment is considered to investigate the general performance of the continuum damage model, with the known values of material properties and structural resistance. Figure 4(a) compares the numerically predicted responses with the experimental results of Brühwiler and Saouma (1991). Two finite element meshes provide similar results, and these are slightly stiffer than the experimental response in the CMOD range of 0.05-0.50 mm. Nonetheless, the present damage mechanics model appears to provide an adequate simulation of the overall structural behaviour, in absence of pore water pressure in the FPZ.

5.2 Simulation of the poro-fracture response of concrete

The two finite element meshes of Fig. 3 provide almost identical responses, and the responses of the refined model are discussed in this

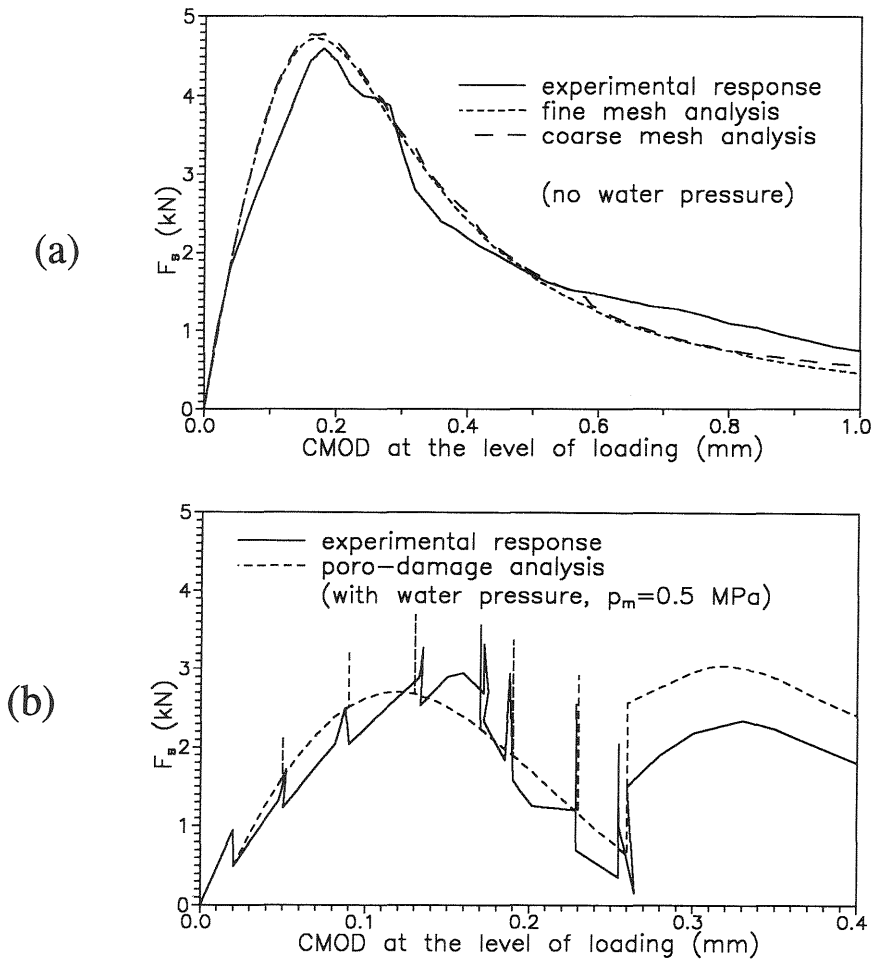


Fig. 4 Numerical simulation of the experimental results (Brüwiler and Saouma 1991): (a) no water pressure, (b) with water pressure

section. The first poro-fracture analysis is conducted with an incremental application of water pressure only, and the specimen fails under an applied pressure of 1.3 MPa. However, this value can not be verified since no experimental result is available on specimens failing under water pressure alone. The laboratory test case with $p_m = 0.5$ MPa is considered next for numerical experiments. The water pressure p_m was applied and released several times in the laboratory, and the specimen was eventually failed with wedge splitting mechanical load, F_s . The CMOD at the level of loading was monitored and the load F_s was adjusted under the changing water pressure and CMOD responses. The indirect displacement control algorithm has been used in the present analyses to adjust the applied load

F_s for the changes in hydrostatic pressure and the CMOD response. Experimental and numerically predicted responses are compared in Fig. 4(b). The overall responses are in good agreement with each other. However, the numerical response is in general slightly stiffer than the experimental response. A substantial difference occurs after the final release of the water pressure at CMOD of 0.26 mm. The numerical analysis shows a higher mechanical resistance before the failure of the specimen. Similar behaviour is observed when responses are compared for the test cases of $p_m=0.3$ MPa and 0.9 MPa (not shown here). The discrepancy after the final release of the water pressure seems to increase with an increasing amplitude of p_m . Some improvements could be made by adjusting the values of b_0 and d_0 within a physically meaningful range. However, such parametric adjustment of the numerical results can be performed only for known experimental conditions, and the general application of the numerical model will be still subjected to uncertainties.

The water pressure in the FPZ might have caused additional micro-structural damage that resulted in a reduced mechanical resistance of the laboratory specimen. The existence of residual water pressure in the FPZ might also have contributed to an apparent reduction of the mechanical resistance. A transient coupled analysis model is required to investigate these aspects of the poro-fracture response of concrete.

6 Conclusions

The poro-damage model appears to provide a reasonable simulation of the water-fracture interactions in the fracture process zone of concrete. However, the damage induced by water pressure seems to be higher in the experimental response. A better correlation between the experimental and numerical responses could be obtained by adjusting the poro-fracture model parameters. Additional micro-mechanical damage caused by the pore-water pressure, that are not reproduced by the effective stress-strain model, may be considered by adjusting the specific fracture energy of concrete. However, more experimental investigations should be conducted before any such empirical adjustments are made in the fracture resistance parameters.

Acknowledgement

The authors are thankful to the Natural Sciences and Engineering Research Council of Canada, Hydro-Québec, Alcan, and the Canadian Electrical Association for supporting this research work at École Polytechnique.

References

- Amadei, B., Illangasekare, T. and Chinnaswamy, C. (1991) Effect of crack uplift on concrete dam stability. **Proceedings of the First Conference on Research Needs in Dam Safety**, New Delhi, Balkema, I, 60-66.
- Ayari, M.L. (1988) Static and dynamic fracture mechanics of concrete gravity dams. Ph.D. Thesis, Dept. of Civil, Env. & Arch. Engg., University of Colorado, Boulder, USA.
- Bhattacharjee, S.S. (1995) FRAC_DAM: a computer program to predict the fracture and damage response of solid concrete structures. Internal Report, Dept. of Civil Engg., Ecole Polytechnique, Montreal, Canada.
- Bhattacharjee, S.S. and Léger, P. (1995) Fracture response of gravity dams due to a rise of the reservoir elevation. **ASCE J. of Struc. Eng.**, 121 (9), (in press).
- Bourdarot, E. and Barry, B. (1994) Effects of temperature and pore pressure in the nonlinear analysis of arch dams, in **Dam Fracture & Damage** (eds E. Bourdarot, J. Mazars and V. Saouma), Balkema, Rotterdam, 187-193.
- Brühwiler, E. and Saouma, V. (1991). Water fracture interaction in cracked concrete dams, **Proceedings of the International Conference on Dam Fracture**, Boulder, Colorado, USA, 553-568.
- Cervera, M., Oliver, J. and Galindo, M. (1992). Numerical analysis of dams with extensive cracking resulting from concrete hydration: simulation of a real case. **Dam Engineering**, 3(1), 1-22.
- Fauchet, B., Coussy, O., Carrère, A., and Tardieu, B. (1991) Poroplastic analysis of concrete dams and their foundations. **Dam Engineering**, II(3), 165-192.
- Ghrib, F. and Tinawi, R. (1995) Nonlinear behaviour of concrete dams using damage mechanics. **ASCE J. of Engg. Mech.**, 121(4), 513-527.
- Gioia, G., Bažant, Z.P., and Pohl, B.H. (1992) Is no-tension dam design always safe? - a numerical study. **Dam Engineering**, 3(1), 23-34.
- Ingraffea, A.R. (1990) Case studies of fracture in concrete dams. **Engineering Fracture Mechanics**, 35(1/2/3), 553-564.
- Linsbauer, H.N., Ingraffea, A.R., Rossmanith, H.P., and Wawrzynek, P.A. (1989) Simulation of cracking in large arch dam: part I & part II. **ASCE J. of Struc. Engg.**, 115(7), 1599-1615 & 1616-1630.
- Reich, R.W., Brühwiler, E., Slowik, V., and Saouma, V.E. (1994) Experimental and computational aspects of a water/fracture interaction, in **Dam Fracture & Damage** (eds E. Bourdarot, J. Mazars and V. Saouma), Balkema, Rotterdam, 123-131.